

Catalytic Micropumps: Microscopic Convective Fluid Flow and Pattern Formation

Timothy R. Kline, Walter F. Paxton, Yang Wang, Darrell Velegol,^{*,†} Thomas E. Mallouk,^{*} and Ayusman Sen^{*}

Department of Chemistry and Center for Nanoscale Science, and Department of Chemical Engineering, Materials Research Institute, The Pennsylvania State University, University Park, Pennsylvania 16802

Received September 2, 2005; E-mail: tom@chem.psu.edu; asen@psu.edu

Scaling a chemistry laboratory down to microchip size is one of the driving forces for developing micro/nanofluidics. Engineering fluid flows at this scale remains an interesting challenge. Flow can be driven by externally applied pressure,¹ electric fields,² thermal³ or concentration gradients.⁴ Heterogeneous catalysis offers a new and potentially powerful alternative. Energy from a “fuel” can be converted locally at a catalyst surface, possibly eliminating external pumps or power sources. We previously reported the autonomous movement of platinum–gold nanorods and micro-gears in dilute solutions of H₂O₂.^{5–8} By Galilean invariance, one should expect immobilized catalytic objects to generate flow in the surrounding fluid, with similar scaling of device size and fluid velocity. Here, we describe pattern formation and convective fluid flow at the microscale induced by the bipolar electrocatalytic decomposition of hydrogen peroxide.

The top image in Figure 1 illustrates flow-induced patterns in a dilute H₂O₂ solution above a gold surface that was patterned with 6–120 μm diameter silver circles and rings; 1.8 μm diameter carboxylated polystyrene spheres were used as tracers to follow the flow of fluid above the catalytic surface. The snapshot in Figure 1 (top), acquired 5 min after adding a suspension of spheres to a thin layer cell with the patterned Ag/Au catalyst surface on the bottom, shows that the particles concentrate in regions between the silver islands. Benard first observed such convection patterns when fluids were perturbed with thermally induced gradients.⁹ This later became known as Marangoni convection, which arises to minimize fluid stresses created by thermal and concentration gradients.^{10,11}

To understand the mechanism of catalytically induced flow, we performed experiments with isolated silver features on gold, and with silver disks separated from the gold underlayer by a film of insulating SiO₂. Gold nanorods, silica spheres, carboxylated polystyrene spheres, and amidine-coated polystyrene spheres were used to study the effects of tracer charge and density.

Figure 1 (bottom) shows trajectories for 2 μm long gold rods and 2 μm diameter amidine-functionalized polystyrene spheres. In both cases, the particles move along the gold surface toward the silver disk or ring. As they approach the silver island, they are swept upward and away in a “back flip” motion (see videos in Supporting Information). The more buoyant spheres (1.050 g/mL) are swept 10–15 μm upward at the edge of the silver disk and then outward as they slowly sediment to the plane of the gold (video I). The less buoyant gold rods (19 g/mL) also circulate at a speed of ~8 μm/s but in a much tighter loop (video II). Figure 1 shows the transiently periodic motion in the radial direction of a gold rod near the silver ring. Because the rods are swept inward from farther away, they concentrate around the silver islands on a time scale of minutes.

An interesting variant of this motion was found for carboxylated polystyrene and silica tracers that are negatively charged in the pH

5.7 H₂O₂ solution. Instead of moving to the edge, these tracers form ring patterns around the silver (video III). Adding 1 mM NaNO₃ greatly reduces both the apparent flow rate and the formation of the ring patterns. If silver is deposited on an insulator, such as glass, no flow or pattern formation is observed, and the tracers no longer avoid the silver features. In contrast, with silver on gold, the upward convective flow prevents tracers from reaching the silver islands.

In our earlier studies of platinum/gold nanorods, we found that catalytically generated interfacial tension gradients could quantitatively account for their axial movement. However, it would be difficult to explain the loss of convective flow when a layer of insulator is interposed between silver and gold on the basis of the interfacial tension model. The strong dependence of flow rate on salt concentration suggests an electrokinetic mechanism for fluid flow.¹⁴ Similar colloidal pattern formation has been seen in electrochemically driven (but noncatalytic) systems.^{12,13} Mano and Heller described proton-flux driven electrokinematic motion of carbon fibers in a cell with a glucose electrooxidizing anode and an O₂ electroreducing cathode.¹⁴

The decomposition of the “fuel”, H₂O₂, to water and oxygen (reaction 1) can be written as the sum of half-cell reactions 2 and 3. The overall reaction 1 has the highly spontaneous cell potential of +1.1 V. It can proceed electrochemically if there is an imbalance in the electrocatalytic activity of the two metals.

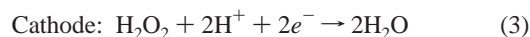


Figure 2 shows a model for electrokinetically driven flow in this system. The observed direction of flow suggests that silver is the cathode in the reaction, reducing H₂O₂ to H₂O and consuming protons (H⁺) in the process; at the anode (gold), H₂O₂ is oxidized, generating protons. Decomposition of H₂O₂ thus creates a proton gradient in the solution above the metal.

Three effects contribute to the motion of the tracer particles: (a) electrophoresis of the particle, (b) the in-plane electroosmotic flow that carries the particles (like a person swimming in a river), and (c) the 3-d flow field resulting from fluid continuity. From the Nernst–Planck equation, an expression for the electric field *E* across the double layer can be derived, where *k*, *T*, *J*₊, *z*, *e*, *D*₊

$$E = \frac{kTJ_+}{z^2eD_+n_\infty} \quad (4)$$

and *n* are the Boltzmann constant, temperature, proton flux obtained from the current density (3.1 × 10⁻⁷ mol/s·m), proton charge, elementary charge, proton diffusion coefficient (9.3 × 10⁻⁹ m²/s), and the proton concentration (2 × 10⁻⁶ M), respectively. To estimate

[†] Department of Chemical Engineering.

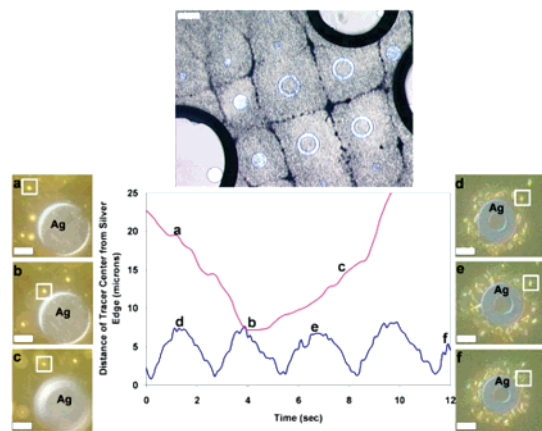


Figure 1. Top: Pattern formation of $1.8 \mu\text{m}$ negatively charged polystyrene spheres (which appear dark in the image) on a silver-patterned gold surface in 0.1% H_2O_2 solution after approximately 5 min. The large circles in the image are oxygen bubbles. Scale bar represents $100 \mu\text{m}$. Bottom: Movement of amidine-functionalized spheres toward a Ag disk (a–b) and away from Ag into a higher plane of focus (c, notice that the substrate is out of focus). The convection-driven periodic motion of $2 \mu\text{m}$ Au rods is illustrated in a plot of the radial displacement of one rod versus time (bottom trace, d–f). Points a–f in the plots refer to the images of sphere and rod motion on the left and right. Scale bar represents $10 \mu\text{m}$.

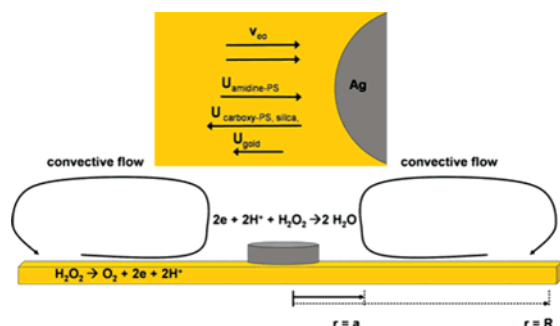


Figure 2. Protons (H^+) generated by oxidation of H_2O_2 migrate from the anode (gold) to cathode (silver, center), generating electroosmotic flow. This flow creates a convection roll that sweeps tracer particles inward along the gold surface. The convection roll extends from $r = a$ (near the silver) to $r = R$. Positively charged tracer particles (see inset) experience an additional electrophoretic force in the direction of the silver island. Negatively charged particles (inset) experience an electrophoretic force in the opposite direction, which results in circular patterns around the silver islands. Gold rods, which experience only a small outward electrophoretic force, are swept inward by the dominant electroosmotic flow and circulate in a tight convection roll near the silver island.

J , we measured the current between gold and silver fingers spaced $10 \mu\text{m}$ apart on an interdigitated microelectrode in 0.5% H_2O_2 .¹⁵ From eq 4, E is $\sim 4.3 \text{ V/cm}$ across the double layer, and we expect a similar magnitude radially. Equation 4 is consistent with literature expressions for E fields produced by ion gradients. An electroosmotic velocity (v_{eo}) of $\sim 8 \mu\text{m/s}$ is calculated from eq 5

$$v_{\text{eo}} = \frac{-\epsilon\zeta_{\text{w}}E}{\eta} \quad (5)$$

where ϵ , ζ_{w} , and η are the permittivity of water, the substrate zeta potential (-25 mV for a planar gold surface¹⁶), and the solution viscosity, respectively.

The same E field that drives electroosmotic flow also causes particle electrophoresis at a rate U_{ep} , where ζ_{p} is the zeta potential on the particle. From eq 6, we see that electrophoresis moves a

$$U_{\text{ep}} = \frac{\epsilon\zeta_{\text{p}}E}{\eta} \quad (6)$$

positively charged particle toward the silver cathode and a negatively charged particle away from it. The total particle velocity (U) is thus $U = v_{\text{eo}} + U_{\text{ep}}$. Positively charged particles (such as amidine-functionalized spheres with $\zeta_{\text{p}} = +40 \text{ mV}$) move inward, as both v_{eo} and U_{ep} are directed inward. Using $E \approx 4 \text{ V/cm}$, the expected amidine particle electrophoretic velocity is $U_{\text{ep}} = 11 \mu\text{m/s}$. The total velocity should be $19 \mu\text{m/s}$ close to the silver disk, consistent with experiment ($\sim 17 \mu\text{m/s}$).

Gold rods—although negatively charged—are also transported inward. The rods have $\zeta_{\text{p}} = -7 \text{ mV}$, which is less negative than that of the carboxylated polystyrene, meaning that electroosmosis (inward) “wins” over electrophoresis (outward). When particles reach either the silver disk ($r = a$) or the edge of the convective region ($r = R$), the bulk flow field set up by the electroosmotic flow comes into play. At the disk, continuity requires that the fluid move upward and then outward. As a result, the amidine and gold particles are transported upward and outward before they reach the silver disk. Since gold is very dense, it makes smaller “loops” than the amidine-functionalized polystyrene (Figure 1).

Negatively charged tracers ($\zeta_{\text{p}} = -60 \text{ mV}$ for carboxylated polystyrene) are transported outward by electrophoresis. The electroosmotic flow is inward, and continuity requires that the bulk fluid come inward from the region $r > R$. As a result of these opposing forces, the particles form a circular pattern a few microns away from the silver feature, as shown in the Supporting Information.

In conclusion, we have demonstrated fluid convection and pattern formation of colloids using a catalytic electrochemical reaction. The system operates on a familiar biomimetic principle, which is to use catalysis to generate a proton gradient. Because galvanic electrochemistry encompasses many chemical reactions, including numerous battery couples, enzymatically coupled redox reactions, such as glucose–oxygen and fuel cell reactions, there is significant potential for using the stored chemical energy of fuels to induce sustained flow in a variety of fluid microsystems.

Acknowledgment. T.E.M. thanks D. Vanderbilt for the suggestion of adapting catalyzed motion to the problem of pumping fluids. This work is supported by the Penn State Center for Nanoscale Science (NSF-MRSEC, DMR-021362), and was performed in part at the Penn State Nanofabrication Facility, a member of the NSF National Nanofabrication Users Network.

Supporting Information Available: Derivation of eq 4 and videos showing (a) the convective motion of positively charged polystyrene spheres (video I) and gold nanorods (video II), and (b) pattern formation by negatively charged polystyrene spheres (video III). This material is available free of charge via the Internet at <http://pubs.acs.org>.

References

- (1) Van Lintel, H. T. G.; Van De Pol, F. C. M.; Bouwstra, S. *Sens., Actuators* **1988**, *15*, 153–67.
- (2) Gallardo, B. S.; Gupta, V. K.; Eagerton, F. D.; Jong, L. I.; Craig, V. S.; Shah, R. R.; Abott, N. L. *Science* **1999**, *283*, 57–60.
- (3) Dawn, E.; Troian, K.; Troian, S. *Nature* **1999**, *402*, 794–7.
- (4) Anderson, J. L. *Annu. Rev. Fluid Mech.* **1989**, *21*, 61–99.
- (5) Paxton, W. F. et al. *J. Am. Chem. Soc.* **2004**, *126*, 13242–31.
- (6) Kline, T. R.; Paxton, W. F.; Mallouk, T. E.; Sen, A. *Angew. Chem., Int. Ed.* **2005**, *44*, 744–6.
- (7) Catchmark, J. M.; Subramanian, S.; Sen, A. *Small* **2005**, *1*, 202–6.
- (8) Paxton, W. F.; Sen, A.; Mallouk, T. E. *Chem.—Eur. J.* **2005**, *11*, 6462–70.
- (9) Benard, H. *Gen. Sci. Pure Appl.* **1900**, *11*, 1261.
- (10) Schtaz, M. F.; VanHook, S. J.; McCormick, W. D.; Swift, J. B.; Swinney, H. L. *Phys. Rev. Lett.* **1995**, *75*, 1938–41.
- (11) Chen, K. P. *Phys. Rev. Lett.* **1997**, *78*, 4395–7.
- (12) Hayward, R. C.; Saville, D. A.; Aksay, I. A. *Nature* **2000**, *404*, 56–9.
- (13) Smith, R.; Prieve, D. C. *Chem. Eng. Sci.* **1982**, *37*, 1203–23.
- (14) Mano, N.; Heller, A. *J. Am. Chem. Soc.* **2005**, *127*, 11574.
- (15) Bard, A. J.; Faulkner, L. R. *Electrochemical Methods: Principles and Applications*, 2nd ed.; John Wiley and Sons: New York; pp 139–144.
- (16) Giesbers, M.; Mieke Kleijn, J.; Cohen Stuart, M. A. *J. Colloid Interface Sci.* **2002**, *248*, 88–95.

JA056069U